Afyon Kocatepe Üniversitesi Fen ve Mühendislik Bilimleri Dergisi
Afyon Kocatepe University – Journal of Science and Engineering
https://dergipark.org.tr/tr/pub/akufemubid

Araştırma Makalesi / Research Article
DOI: https://doi.org/10.35414/akufemubid.1407387
AKÜ FEMÜBİD **24** (2024) 041101 (782-788)
AKU J. Sci. Eng. **24** (2024) 041101 (782-788)

Numerical Analysis of Highly Sensitive D-Shaped PCF SPR Temperature Sensor

Makale Bilgisi / Article Info
Alındı/Received: 20.11.2023
Kabul/Accepted: 13.06.2024
Yayımlandı/Published: 20.08.2024

Yüksek hassasiyetli D Şekilli PCF SPR Sıcaklık Sensörünün Sayısal Analizi

İlhan ERDOĞAN * **, Yusuf DOĞAN**

Sivas University of Science and Technology, Faculty of Engineering and Natural Sciences, Electrical and Electronics Engineering, Sivas, Türkiye

Abstract

This numerical study presents an investigation of an optical fiber D-shaped PCF SPR sensor for temperature sensing, via the finite element method-based COMSOL Multiphysics simulation software. In the proposed PCF configuration, the sensor consists of two different-sized air holes and a gold layer. Between 10°C and 60°C, pure ethanol and an ethanol-chloroform mixture are selected to be used as analytes and their temperature sensitivities are compared. The effect of sensor parameters on sensor sensitivity is studied, and the optimum value is set for each parameter. The maximum sensitivity is calculated as 2008 pm/°C for the pure ethanol, while it has reached 7750 pm/°C for the ethanol-chloroform mixture, showing that chloroform improves the performance. The sensor proposed in this study has a higher temperature sensitivity compared to other studies and therefore has significant potential for applications requiring precise measurement.

Keywords: Surface plasmon resonance (SPR); Finite element method (FEM); Fiber optic sensors; Photonic crystal fiber (PCF); Temperature sensor.

Öz

Bu sayısal çalışma, sonlu elemanlar yöntemi tabanlı COMSOL Multiphysics simülasyon yazılımıyla sıcaklık algılama için optik fiber D-şekilli PCF SPR sensörünün bir incelemesini sunmaktadır. Önerilen PCF konfigürasyonunda sensör, iki farklı boyutta hava boşlukları ve bir altın katmandan oluşmaktadır. 10°C ile 60°C arasında, analit olarak kullanılmak üzere saf etanol ve etanol-kloroform karışımı seçilmiş ve sıcaklık duyarlılıkları karşılaştırılmıştır. Sensör parametrelerinin sensör hassasiyeti üzerindeki etkisi incelenmiş ve her parametre için optimum değer belirlenmiştir. Maksimum hassasiyet saf etanol için 2008 pm/°C olarak hesaplanırken, etanol-kloroform karışımı için 7750 pm/°C değerine ulaşmıştır, bu da kloroformun performansı artırdığını göstermektedir. Bu çalışmada önerilen sensör, diğer çalışmalara kıyasen daha yüksek sıcaklık hassasiyetine sahip olduğundan hassas ölçüm gerektiren uygulamalar için önemli bir potansiyele sahiptir.

Anahtar Kelimeler: *Yüzey plazmon rezonans (SPR); Sonlu elemanlar yöntemi (FEM); Fiber optik sensörler; Fotonik kristal fiber (PCF); Sıcaklık sensörü.*

1. Introduction

Surface plasmon resonance (SPR) is an optical phenomenon that is associated with the massive release of electrons called plasmons that take place at the boundary between a dielectric material and a metal (Erdogan & Dogan, 2023). SPR is commonly preferred sensing applications such as chemical (Moznuzzaman et al., 2020), physical (Chaudhary et al., 2022), and biochemical (Chaudhary et al., 2022; Liu & Peng, 2020) due to its advantages of the ability to be extremely sensitive to the little alterations in the refractive index (RI) of the surrounding environment. SPR-based sensors have been widely employed for many different purposes such as RI sensing (Dogan & Erdogan, 2023; Dogan et al., 2023), food quality detection (Yadav et al., 2020; Zhou et al., 2019), pressure (Zhao et al., 2019), temperature measurement (Chao et al., 2023; Zhao et al., 2019), biochemical (Kumar et al., 2022), and gas detection (Kumar et al., 2022; Liu et al., 2021). Optical fiber SPR sensors provide some advantages, such as easy integration and fabrication, remote sensing capabilities, compact size, and cost-effective production compared with prism-based ones (Wang et al., 2022). SPR sensors are vital for sensing applications and there are studies on different structures such as V-shaped (Abdelghaffar et al., 2023), D-shaped (Dogan et al., 2023; Erdogan & Dogan, 2023; Gangwar & Singh, 2017), tapered fiber (D. Wang et al., 2021), and U-bend (Xie et al., 2021). In the SPR sensors, metals such as silver, gold, nickel, and copper have been used as highly sensitive plasmonic layers thanks to their have many charge carriers. Moreover, in general, because of resistance to oxidation and chemical stability, silver and gold have been preferred as plasmonic layers (Pandey et al., 2023). Plastic optical fiber, photonic crystal fiber (PCF), multi-mode fiber, and single-mode fiber are different fiber optics types and these are used in

*Sorumlu Yazar/Corresponding Author: İlhan ERDOĞAN e-posta/e-mail: ilhan.erdogan@sivas.edu.tr

different SPR sensor applications. Compared to conventional optical fibers and other types of sensors, PCF sensors offer some important advantages, such as enhanced light-guiding properties, design flexibility, high sensitivity, large evanescent field, and compact size (Abdelghaffar et al., 2023; Ramola et al., 2021). PCF air holes can be produced through the stack-and-draw method (Amouzad Mahdiraji et al., 2014). D-shaped fibers have significant advantages, like being easy to manufacture via side polishing technique (Chen et al., 2016) and achieving significant evanescent field effects (An et al., 2017). By chemical vapor deposition (CVD) or sputtering technology, the gold layer can be deposited on the surface of a D-shaped PCF (Abbas & Mahdi, 2023; Zhou et al., 2014). In PCF, the air holes confine the light to a specific area and provide an effective coupling between surface plasmon polaritons (SPP) and core modes. In this study, the main motivation is to integrate the advantages of the PCF structure and D-shaped fiber.

In this work, a D-shaped SPR PCF temperature sensor with a gold layer is investigated by finite element method (FEM) based COMSOL Multiphysics. To examine the performance of the proposed sensor, the electric field intensity distribution, and the confinement loss have been studied with the effect of the diameter of the air holes, gold thickness, and polishing depth on sensitivity. The proposed D-shaped SPR-PCF sensor shows finely temperature sensitivity and linearity.

2. Design and Theoretical Background

In this study, a D-shaped PCF SPR sensor has been designed for temperature sensing. The sensitivity of the sensor depends on four parameters: d1-factor (d1/Λ), d2-factor (d2/d1), h-factor(h/d1), and Au_th. Hole-to-hole spacing (Λ) is fixed at 4 µm. The diameters of large and small air holes are mentioned as d1 and d2, respectively. PCF sensor consists of air holes. It used air holes in this D-shaped PCF SPR sensor structure to achieve greater light confinement in the core region. Figure 1 illustrates a 2D cross-sectional of the designed SPR sensor using D-shaped PCF. Sensitivity performance can be further improved by optimizing sensor parameters as described in Section 3.

FEM-based COMSOL Multiphysics software is employed for the numerical examination to investigate the characteristics of the propagation of light. In FEM numerical analysis, physics-controlled mesh elements are employed to discretize the entire geometry and boundaries of the PCF structure.

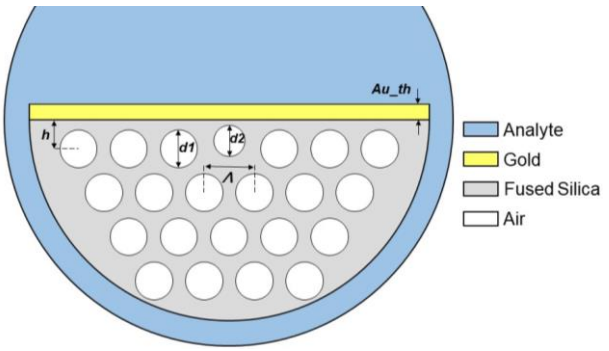

Figure 1. Proposed D-shaped SPR-PCF 2D view

The software's mode analysis is utilized to investigate and figure out the effective mode index for the pertinent modes. SPP waves emerge when the phase-matching condition is satisfied upon the interaction of polarized light with a metal-dielectric layer. Eq. 1 illustrates this matching condition (Nayak & Jha, 2017):

$$k_{SP} \approx \frac{w}{c}\left(\frac{\epsilon_m \epsilon_s}{\epsilon_m + \epsilon_s}\right)^{1/2} \quad (1)$$

Where k, c, ω, ϵm, and ϵs are phase, the light's speed, angular frequency, metal's dielectric constant, and the dielectric medium's constant, respectively. The Sellmeier equation is employed, as expressed in Eq. 2, to calculate the RI of silica. (Haque et al., 2018):

$$n_1(\lambda) = \left(1 + \frac{a_1\lambda^2}{\lambda^2 - {b_1}^2} + \frac{a_2\lambda^2}{\lambda^2 - {b_2}^2} + \frac{a_3\lambda^2}{\lambda^2 - {b_3}^2}\right)^{1/2} \quad (2)$$

In the equation, a_1, a_2, a_3, b_1, b_2, and b_3 are Sellmeier parameters which 0.6961663, 0.4079426, 0.8974794, 0.0684043 µm, 0.1162414µm, 9.896161µm, respectively. Au the layer's dispersion relation is established using the Drude model, and the associated equation is presented in Eq. 3 (Sharma & Gupta, 2007).

$$\epsilon_m(\lambda) = \epsilon_{mr} + i\,\epsilon_{mi}; \quad = 1 - \left(\frac{\lambda^2\lambda_c}{{\lambda_p}^2(\lambda_c + i\lambda)}\right) \quad (3)$$

Here, the values of λp and λc for gold (Sharma & Gupta, 2007) are 0.16826 µm and 8.9342 µm, respectively. For the mixture of ethanol/ chloroform, Eq. 4 illustrates the correlation between temperature and RI (Xu et al., 2008; Zhang et al., 2021).

$$n_T = x\% \left[n_{ethanol_{T=20\,℃}} + \frac{dn_{ethanol}}{dT}(T-20) \right] + (100-x)\% \left[n_{chloroform_{T=20\,℃}} + \frac{dn_{chloroform}}{dT}(T-20) \right] \quad (4)$$

In this equation, x stands for the rate of the ethanol/chloroform. In the SPR sensors, confinement loss is mostly used to interpret the characteristics of sensors. A lot of the energy in the core domain of the fiber to the metal surface is connected, and the core region's energy decreases. This optical phenomenon can be calculated using the Eq. 5 (Yang et al., 2011).

$$Loss = \frac{40\pi Im(n_{eff})}{\ln(10)\,\lambda} 10^4 \approx 8.686\,\frac{2\pi}{\lambda} Im(n_{eff}) 10^4\ [db/cm] \quad (5)$$

In this equation, λ shows the wavelength (μm), and Im(neff) denotes the mode index's imaginary part dependent on core-guided modes. Additionally, a crucial parameter under consideration is the change in resonance wavelength (λres) associated with temperature variations (ΔT). The primary emphasis of this investigation is on sensitivity (S) defined by Eq. 6:

$$S = \frac{\Delta\lambda_{res}}{\Delta T} \quad (6)$$

3. Results and Discussions

In this numerical study, a fiber optic D-shaped PCF SPR sensor structure is created for temperature sensing and numerically examined in the FEM. In the proposed sensor, there are four parameters as d1-factor, d2-factor, h-factor, and Au_th that are swept in the range of 0.5-0.8, 0.35-0.50, 0.6-0.9, and 45-65 nm, respectively. These values are determined considering the physical limitations of the PCF sensor structure and the range where surface plasmon appear. Figure 2 shows the relation between the change in wavelength and confinement loss with the real effective RI of core and SPP modes and the e-field distribution of these modes for the mixture of ethanol and chloroform at 60 ℃. For this sensor to provide maximum sensitivity, it is essential to optimize the parameters. The refractive indices corresponding to 30℃ and 60℃ analytes are calculated from Eq. 4.

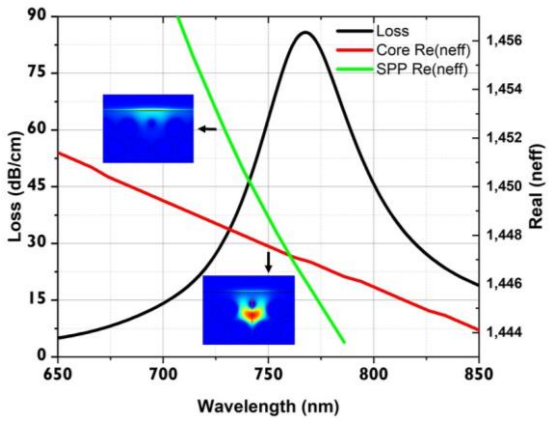

Figure 2. Confinement loss and the real effective refractive indices of the SPP and Core modes in a mixture of ethanol and chloroform at 60 °C vs. wavelength, and electric field distribution for both modes

In the optimization process, one input is swept while others are kept constant, which is reiterated for each parameter. As shown in Figure 3a, the d1-factor is swept between 0.5 and 0.8 with 0.1 increments, and the sensor sensitivity is observed to get higher as the d1-factor increases. The maximum sensitivity has reached 2546.33 pm/°C at 0.8 d1-factor. Figure 3b depicts the d2-factor, which is swept between 0.35 and 0.50 with 0.05 increments, and the sensitivity gets slightly lower with the increasing d2-factor. The maximum sensitivity is 2546.33 pm/°C when the d2-factor is 0.35.

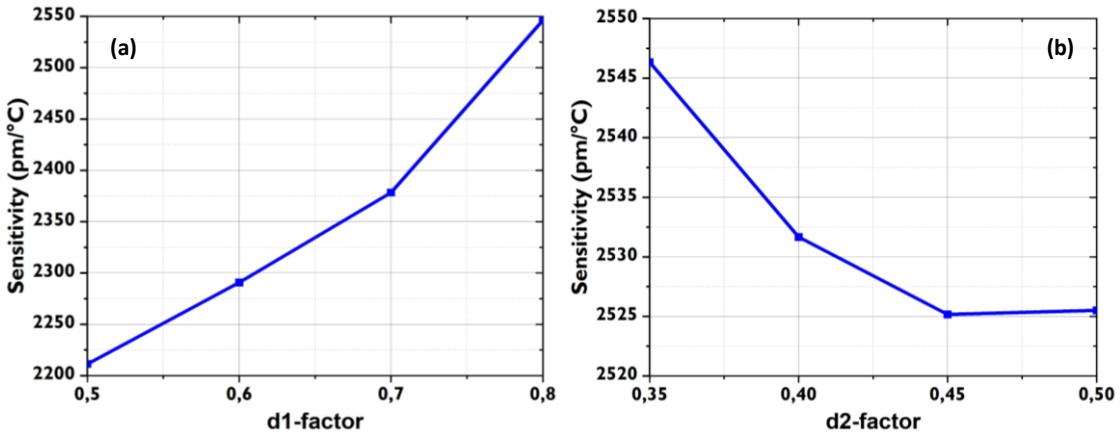

Figure 3. Sensitivity for d1 factor and d2 factor in the different ranges.

The h-factor is varied between 0.6 and 0.9 with 0.1 increments, and the sensitivity tends to go up as the h-factor increases and reaches the highest point at h-factor 0.9 with a value of 2962.66 pm/°C, as seen in Figure 4. As can be comprehended from the figure, the distance between the metal layer and the fiber core has a dramatic effect on the sensitivity.

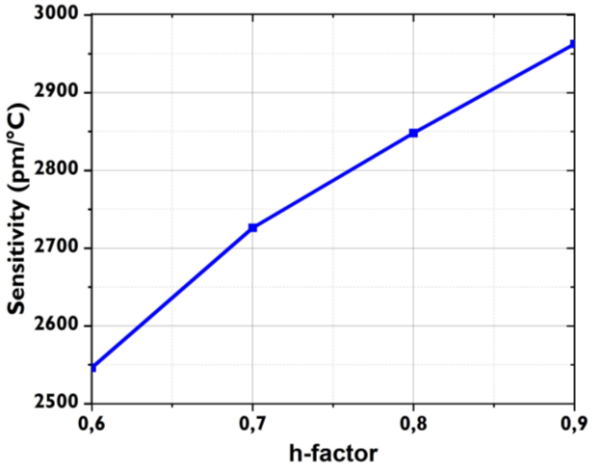

Figure 4. Sensitivity for h-factor in the different ranges.

After optimizing the d1-factor, d2-factor, and h-factor, the Au_th parameter is swept from 45 nm to 65 nm. Table 1 shows that the peak sensitivity of 3000.34 pm/°C is reached at 55 nm Au_th. It is observed that the metallic layer thickness influences the coupling between the core and surface plasmonic modes. As a result, the optimum values of d1-factor, d2-factor, h-factor, and Au_th parameters in the sensor structure are 0.8, 0.35, 0.9, and 55 nm, respectively.

Table 1. Sensitivity corresponding to Au_th of 45, 55, and 65 nm

Au_th (nm)	*h-factor*	*d2-factor*	*d1-factor*	*Sensitivity (pm/°C)*
45	0.9	0.35	0.8	2962.66
55	0.9	0.35	0.8	3000.34
65	0.9	0.35	0.8	2922.5

The confinement loss has been calculated for the mixture of ethanol and chloroform at various degrees, as seen in Figure 5. It is understood that both the confinement loss and the resonant wavelength decrease as the temperature increases. Likewise, the confinement loss for pure ethanol at various degrees has been calculated, as seen in Figure 6. It is seen that the confinement loss and the resonant wavelength again decrease with increasing temperature. However, the change in the resonance wavelength is much smaller for given temperature changes when compared to the ethanol chloroform mixture analyte, leading to lower sensitivity.

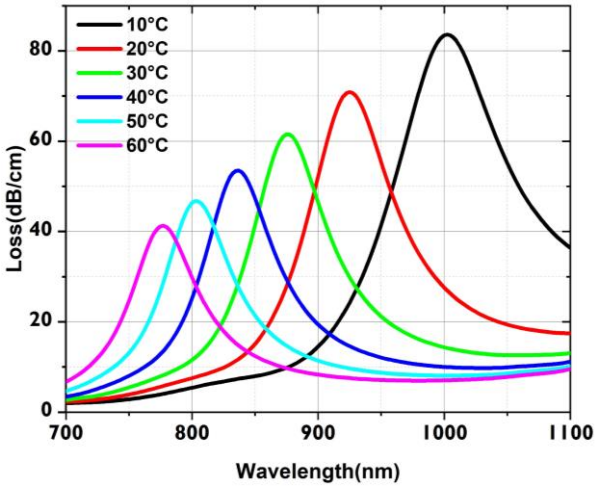

Figure 5. Confinement loss vs resonance wavelength for a mixture of ethanol and chloroform at various degrees

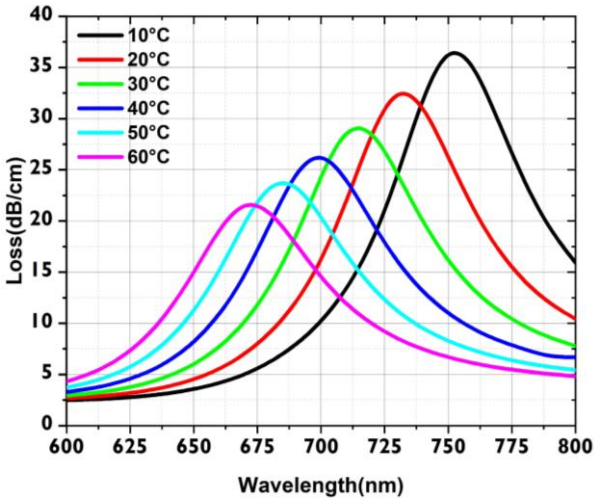

Figure 6. Confinement loss vs resonance wavelength for pure ethanol at various degrees

Figure 7 depicts the correlation between temperature and resonance wavelength for pure ethanol and a mixture of ethanol/chloroform between 10°C and 60°C. For both analytes, the resonance wavelength decreases with increasing temperature between points 1-6. For the mixture of ethanol and chloroform, temperature sensor sensitivity at $S_{1\text{-}2}$, $S_{2\text{-}3}$, $S_{3\text{-}4}$, $S_{4\text{-}5}$, and $S_{5\text{-}6}$ are 7750 pm/°C, 5000 pm/°C, 3850m/°C, 3350 pm/°C, 2580 pm/°C, respectively. For $S_{2\text{-}3}$, ΔT is 10 °C and Δλres is 50 nm, which yields a sensitivity of 5000 pm/°C. The maximum temperature sensitivity has been attained as 7750 pm/°C between 10 and 20 °C. In addition, for pure ethanol, temperature sensitivity at $S_{1\text{-}2}$, $S_{2\text{-}3}$, $S_{3\text{-}4}$, $S_{4\text{-}5}$, and $S_{5\text{-}6}$ are 2008 pm/°C, 1747 pm/°C, 1500 pm/°C, 1445 pm/°C, 1290 pm/°C, respectively. The maximum temperature sensitivity is obtained as 2008 pm/°C between 10 and 20 °C. Adding chloroform to the ethanol solution significantly increases the sensitivity by shifting the resonance wavelength from the region to the near-infrared region.

Table 2: Maximum sensitivity comparison

Sensor Type	Analyte	Temperature [℃]	Max. Sensitivity [pm/℃]	Refs.
Trapezoidal- Shaped SPR-PCF	Ethanol & Chloroform	10-60	5200	(Chao et al., 2023)
PCF SPR	Magnetic fluids	20-80	1410	(Gu et al., 2022)
PCF SPR	PDMS	5-45	3757	(Gao et al., 2023)
CTF-SPR	Ethanol	20-50	3200	(Q. Wang et al., 2021)
Hexagonal PCF	Sea water	30-60	5000	(Abdullah et al., 2020)
D-shaped PCF-SPR	PDMS	25-55	229	(Mo et al., 2021)
D-shaped PCF-SPR	Ethanol & Chloroform Pure ethanol	10-60	7750 2008	Proposed

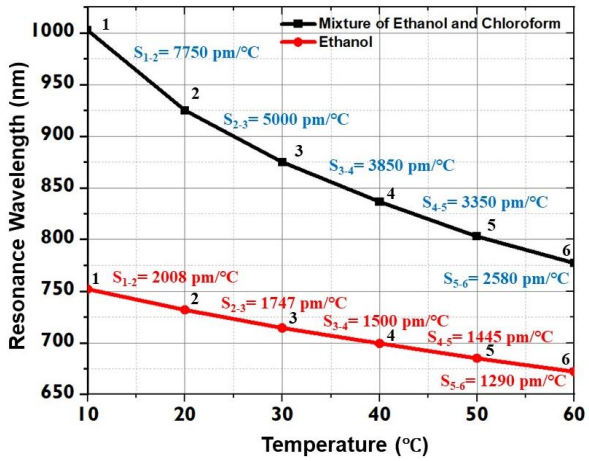

Figure 7. The correlation between sensitivity and resonance wavelength for the two analytes in the temperature range of 10 ℃ to 60 ℃.

Table 2 demonstrates the maximum sensitivity comparison with other works in the literature. The proposed D-shaped PCF-SPR sensor using optical fiber has attained superior sensitivity in temperature measurement.

4. Conclusions

In this work, an optical fiber D-shaped PCF SPR sensor is proposed as a temperature sensor and numerically examined via the FEM-based COMSOL Multiphysics software. The sensor performance has been analyzed for ethanol and an ethanol-chloroform mixture in the temperature range of 10 ℃ to 60 ℃. Four sensor parameters are optimized to reach the highest temperature sensitivity, and the best combination has been found as 0.8, 0.35, 0.9, and 55 nm representing d1-factor, d2-factor, h-factor, and Au_th, respectively. The trend in confinement loss and resonance wavelength have been investigated in reference to temperature. The maximum sensor sensitivity has been acquired as 7750 pm/℃ in the range of 10 ℃-20 ℃ for the mixture of ethanol and chloroform, while it is 2008 pm/℃ for the pure ethanol at the same temperatures. The proposed sensor offers significantly higher sensitivity compared to previous works, which makes it promising for future works.

Declaration of Ethical Standards

The authors declare that they comply with all ethical standards.

Credit Authorship Contribution Statement

Author 1: Research, Analysis, Writing, Figures, Data, Review and Editing.

Author 2: Research, Analysis, Writing, Supervision.

Declaration of Competing Interest

The authors have no conflicts of interest to declare regarding the content of this article.

Data Availability Statement

All data generated or analyzed during this study are included in this published article.

Acknowledgement

This work has been supported by the Scientific Research Projects Coordination Unit of the Sivas University of Science and Technology. Project Number: 2022-GENL-Eng-0001

5. References

Abbas, H. K., & Mahdi, Z. F. J. R. i. O. (2023). Fabricate a highly sensitive surface plasmon resonance optical fiber sensor based on a D-shape fiber coated with gold (Au) nano-layer. *12*, 100497. https://doi.org/10.1016/j.rio.2023.100497

Abdelghaffar, M., Gamal, Y., El-Khoribi, R. A., Soliman, W., Badr, Y., Hameed, M. F. O., & Obayya, S. (2023). Highly sensitive V-shaped SPR PCF biosensor for

cancer detection. *Optical Quantum Electronics*, *55*(5), 472. https://doi.org/10.1007/s11082-023-04740-w

Abdullah, H., Islam, M. R., Ahmed, K., Malka, D., Nguyen, T. K., Hossain, M. N., . . . Dhasarathan, V. (2020). Theoretical analysis of highly temperature-sensitive fem based optical sensor in the infrared range. *Optik*, *205*, 164060. https://doi.org/10.1016/j.ijleo.2019.164060

Amouzad Mahdiraji, G., Chow, D. M., Sandoghchi, S., Amirkhan, F., Dermosesian, E., Yeo, K. S., . . . Optics, I. (2014). Challenges and solutions in fabrication of silica-based photonic crystal fibers: an experimental study. *33*(1-2), 85-104. https://doi.org/10.1080/01468030.2013.879680

An, G., Li, S., Wang, H., & Zhang, X. (2017). Metal oxide-graphene-based quasi-D-shaped optical fiber plasmonic biosensor. *IEEE Photonics Journal*, *9*(4), 1-9. https://doi.org/10.1109/JPHOT.2017.2722543

Chao, C.-T. C., Chen, S.-H., Huang, H. J., Kooh, M. R. R., Lim, C. M., Thotagamuge, R., . . . Chau, Y.-F. C. (2023). Improving Temperature-Sensing Performance of Photonic Crystal Fiber via External Metal-Coated Trapezoidal-Shaped Surface. *Crystals*, *13*(5), 813. https://doi.org/10.3390/cryst13050813

Chaudhary, V. S., Kumar, D., Pandey, B. P., & Kumar, S. (2022). Advances in photonic crystal fiber-based sensor for detection of physical and biochemical parameters-a review. *IEEE Sensors Journal*. https://doi.org/10.1109/JSEN.2022.3222969

Chen, Y., Xie, Q., Li, X., Zhou, H., Hong, X., & Geng, Y. (2016). Experimental realization of D-shaped photonic crystal fiber SPR sensor. *Journal of Physics D: Applied Physics*, *50*(2), 025101. https://doi.org/10.1088/1361-6463/50/2/025101

Dogan, Y., & Erdogan, I. (2023). Highly sensitive MoS2/graphene based D-shaped optical fiber SPR refractive index sensor with Ag/Au grated structure. *Optical Quantum Electronics*, *55*(12), 1-12. https://doi.org/10.1007/s11082-023-05315-5

Dogan, Y., Katirci, R., Erdogan, İ., & Yartasi, E. (2023). Artificial neural network based optimization for Ag grated D-shaped optical fiber surface plasmon resonance refractive index sensor. *Optics Communications*, *534*, 129332. https://doi.org/10.1016/j.optcom.2023.129332

Erdogan, İ., & Dogan, Y. (2023). Au-TiO2-Graphene Grated Highly Sensitive D-Shaped SPR Refractive Index Sensor. *Plasmonics*, 1-8. https://doi.org/10.1007/s11468-023-01847-4

Gangwar, R. K., & Singh, V. K. (2017). Highly sensitive surface plasmon resonance based D-shaped photonic crystal fiber refractive index sensor. *Plasmonics*, *12*, 1367-1372. https://doi.org/10.1007/s11468-016-0395-y

Gao, S., Wei, K., Yang, H., Tang, Y., Yi, Z., Tang, C., . . . Wu, P. (2023). Design of surface plasmon resonance-based D-type double open-loop channels PCF for temperature sensing. *Sensors*, *23*(17), 7569. https://doi.org/10.3390/s23177569

Gu, S., Sun, W., Li, M., Li, Z., Nan, X., Feng, Z., & Deng, M. (2022). Simultaneous measurement of magnetic field and temperature based on photonic crystal fiber plasmonic sensor with dual-polarized modes. *Optik*, *259*, 169030. https://doi.org/10.1016/j.ijleo.2022.169030

Haque, E., Hossain, M. A., Ahmed, F., & Namihira, Y. (2018). Surface plasmon resonance sensor based on modified $ D $-shaped photonic crystal fiber for wider range of refractive index detection. *EEE Sensors Journal*, *18*(20), 8287-8293. https://doi.org/10.1109/JSEN.2018.2865514

Kumar, V., Raghuwanshi, S. K., & Kumar, S. (2022). Recent advances in carbon nanomaterials based spr sensor for biomolecules and gas detection-A review. *IEEE Sensors Journal*. https://doi.org/10.1109/JSEN.2022.3191042

Liu, W., Shi, Y., Yi, Z., Liu, C., Wang, F., Li, X., . . . Chu, P. K. (2021). Surface plasmon resonance chemical sensor composed of a microstructured optical fiber for the detection of an ultra-wide refractive index range and gas-liquid pollutants. *Optics Express*, *29*(25), 40734-40747. https://doi.org/10.1364/OE.444323

Liu, Y., & Peng, W. (2020). Fiber-optic surface plasmon resonance sensors and biochemical applications: a review. *Journal of Lightwave Technology*, *39*(12), 3781-3791. https://doi.org/10.1109/JLT.2020.3045068

Mo, X., Lv, J., Liu, Q., Jiang, X., & Si, G. (2021). A magnetic field SPR sensor based on temperature self-reference. Sensors, *21*(18), 6130. https://doi.org/10.3390/s21186130

Moznuzzaman, M., Islam, M. R., Hossain, M. B., & Mehedi, I. M. (2020). Modeling of highly improved SPR sensor for formalin detection. *Results in Physics*, *16*, 102874. https://doi.org/10.1016/j.rinp.2019.102874

Nayak, J. K., & Jha, R. (2017). Numerical simulation on the performance analysis of a graphene-coated optical fiber plasmonic sensor at anti-crossing. *Applied Optics*, *56*(12), 3510-3517. https://doi.org/10.1364/AO.56.003510

Pandey, P. S., Raghuwanshi, S. K., Singh, R., & Kumar, S. (2023). Surface plasmon resonance biosensor chip for human blood groups identification assisted with silver-chromium-hafnium oxide. *Magnetochemistry*, *9*(1), 21. https://doi.org/10.3390/magnetochemistry9010021

Ramola, A., Marwaha, A., & Singh, S. (2021). Design and investigation of a dedicated PCF SPR biosensor for CANCER exposure employing external sensing. *Applied Physics A*, *127*(9), 643. https://doi.org/10.1007/s00339-021-04785-2

Sharma, A. K., & Gupta, B. (2007). Influence of dopants on the performance of a fiber optic surface plasmon resonance sensor. *Optics Communications*, *274*(2), 320-326. https://doi.org/10.1016/j.optcom.2007.02.030

Wang, D., Li, W., Zhang, Q., Liang, B., Peng, Z., Xu, J., . . . Li, J. (2021). High-performance tapered fiber surface plasmon resonance sensor based on the graphene/Ag/TiO2 layer. *Plasmonics*, *16*(6), 2291-2303. https://doi.org/10.1007/s11468-021-01483-w

Wang, Q., Zhang, X., Yan, X., Wang, F., & Cheng, T. (2021). Design of a surface plasmon resonance temperature sensor with multi-wavebands based on conjoined-tubular anti-resonance fiber. Photonics, https://doi.org/10.3390/photonics8060231

Wang, Z., Zhang, W., Liu, X., Li, M., Lang, X., Singh, R., . . . Kumar, S. (2022). Novel optical fiber-based structures for plasmonics sensors. *Biosensors*, *12*(11), 1016. https://doi.org/10.3390/bios12111016

Xie, T., He, Y., Yang, Y., Zhang, H., & Xu, Y. (2021). Highly sensitive surface plasmon resonance sensor based on graphene-coated U-shaped fiber. *Plasmonics*, *16*, 205-213. https://doi.org/10.1007/s11468-020-01264-x

Xu, Y., Chen, X., & Zhu, Y. (2008). High sensitive temperature sensor using a liquid-core optical fiber with small refractive index difference between core and cladding materials. *Sensors*, *8*(3), 1872-1878. https://doi.org/10.3390/s8031872

Yadav, M. K., Kumar, P., & Verma, R. (2020). Detection of adulteration in pure honey utilizing Ag-graphene oxide coated fiber optic SPR probes. *Food chemistry*, *332*, 127346. https://doi.org/10.1016/j.foodchem.2020.127346

Yang, K.-Y., Chau, Y.-F., Huang, Y.-W., Yeh, H.-Y., & Ping Tsai, D. (2011). Design of high birefringence and low confinement loss photonic crystal fibers with five rings hexagonal and octagonal symmetry air-holes in fiber cladding. *Journal of Applied Physics*, *109*(9). https://doi.org/10.1063/1.3583560

Zhang, Y., Chen, H., Wang, M., Liu, Y., Fan, X., Chen, Q., & Wu, B. (2021). Simultaneous measurement of refractive index and temperature of seawater based on surface plasmon resonance in a dual D-type photonic crystal fiber. *Materials Research Express*, *8*(8), 085201. https://doi.org/10.1088/2053-1591/ac1ae7

Zhao, Y., Wu, Q.-l., & Zhang, Y.-n. (2019). Simultaneous measurement of salinity, temperature and pressure in seawater using optical fiber SPR sensor. *Measurement*, *148*, 106792. https://doi.org/10.1016/j.measurement.2019.07.020

Zhou, J., Qi, Q., Wang, C., Qian, Y., Liu, G., Wang, Y., & Fu, L. (2019). Surface plasmon resonance (SPR) biosensors for food allergen detection in food matrices. *Biosensors Bioelectronics*, *142*, 111449. https://doi.org/10.1016/j.bios.2019.111449

Zhou, W., Mandia, D. J., Griffiths, M. B., Barry, S. T., & Albert, J. J. T. J. o. P. C. C. (2014). Effective permittivity of ultrathin chemical vapor deposited gold films on optical fibers at infrared wavelengths. *118*(1), 670-678. https://doi.org/10.1021/jp410937f